

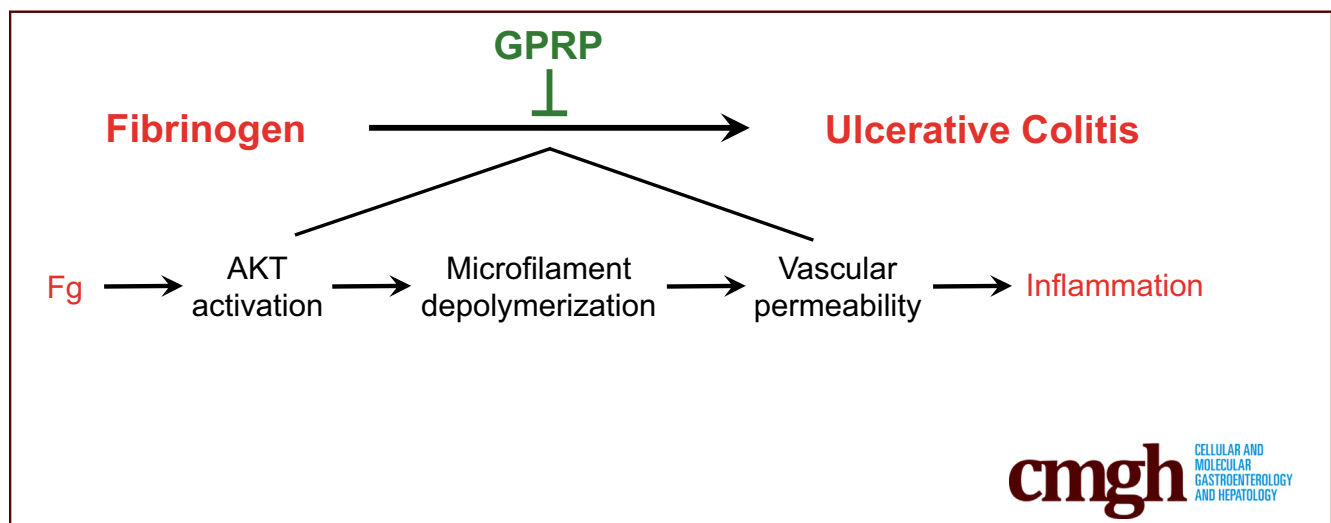
## ORIGINAL RESEARCH

## Fibrinogen/AKT/Microfilament Axis Promotes Colitis by Enhancing Vascular Permeability



Chong Zhang,<sup>1,2,\*</sup> Honglv Chen,<sup>1,\*</sup> Qiaoling He,<sup>1</sup> Yiqin Luo,<sup>1</sup> Andong He,<sup>1</sup> Ailin Tao,<sup>1</sup> and Jie Yan<sup>1</sup>

<sup>1</sup>State Key Laboratory of Respiratory Disease, Guangdong Provincial Key Laboratory of Allergy & Clinical Immunology, Second Affiliated Hospital, Guangzhou Medical University, Guangzhou, China; and <sup>2</sup>Guangxi Key Laboratory of Molecular Medicine in Liver Injury and Repair, Guilin Medical University, Guilin, China



## SUMMARY

Fibrinogen, which was upregulated in human and mouse colitis, promoted colitis by enhancing vascular permeability via activating Akt and subsequent microfilament depolymerization. Targeting fibrinogen may serve as an attractive anti-colitis therapy.

**BACKGROUND & AIMS:** Increased vascular permeability (VP) has been indicated to play an important role in the pathogenesis of inflammatory bowel disease (IBD). However, the pathological causes of increased intestinal VP in IBD remain largely unknown.

**METHOD:** Fibrinogen level was measured in dextran sulphate sodium (DSS)-induced colitis and patients with ulcerative colitis. Gly-Pro-Arg-Pro acetate (GPRP), an Fg inhibitor, was used to detect the effect of Fg inhibition on the pathogenesis of DSS-induced colitis, as indicated by tissue damage, cytokine release and inflammatory cell infiltration. Miles assay was used to detect vascular permeability.

**RESULTS:** Through tandem mass tag-based quantitative proteomics, fibrinogen (Fg) was found to be upregulated in

the colon of DSS-treated mice, which was consistent with increased Fg level in colon sample of patients with ulcerative colitis. Gly-Pro-Arg-Pro acetate (GPRP), an Fg inhibitor, significantly alleviated DSS-induced colitis as indicated by improvement of body weight loss and mortality. GPRP decreased colonic inflammation and VP in DSS-treated mice. *In vivo*, Fg enhanced VP as indicated by Miles assay, which was significantly inhibited by GPRP, AKT (serine/threonine kinase 1) inhibitors and low doses of Jasplakinolide which induced actin polymerization, while was dramatically enhanced by Cytochalasin D (an actin polymerization inhibitor). Moreover, activation of AKT was found in vessels of DSS-treated mice. *In vitro*, Fg induced activation of AKT and depolymerization of microfilament and promoted cell-to-cell disaggregation. Furthermore, inhibition of AKT decreased Fg-induced microfilament depolymerization.

**CONCLUSIONS:** Our findings highlight the importance of Fg in regulating colitis by modulation of VP via activating AKT and subsequent depolymerization of microfilament and suggest Fg as an attractive target for anti-colitis treatment. (*Cell Mol Gastroenterol Hepatol* 2021;11:683–696; <https://doi.org/10.1016/j.jcmgh.2020.10.007>)

**Keywords:** Fibrinogen; Vascular Permeability; Colitis; GPRP Acetate.

Ulcerative colitis (UC), a subtype of inflammatory bowel disease (IBD), is a chronic inflammatory disease that affects the colon. The pathogenesis is multifactorial, involving genetic predisposition, epithelial barrier defects, dysregulated immune responses, and environmental factors.<sup>1</sup> Increased vascular permeability (VP), which is essential for infiltration of inflammatory cells, is one of the main characteristics of inflammation related diseases, including IBD, diabetes, and retinal diseases.<sup>2</sup> Moreover, increased VP precedes epithelial barrier dysfunction in IBD.<sup>3,4</sup> In addition, targeting VP has begun to show preclinical and clinical promise.<sup>2</sup>

Recent studies have shown that increased VP plays an important role in the pathogenesis of UC. Taniguchi et al<sup>5</sup> found that vessels were immature and VP was increased in active inflamed mucosa of UC patients. Similar results are obtained in experimental colitis models. Increased VP is also found in dextran sodium sulfate (DSS) and iodoacetamide-induced UC in rats and mice.<sup>3</sup> Activation of TRPV4 (transient receptor potential vanilloid 4 channel) contributes to colonic inflammation in DSS-induced murine colitis by upregulating vascular endothelial permeability.<sup>6</sup> Interferon gamma (IFN- $\gamma$ ) enhances VP in acute and chronic UC and anti-IFN- $\gamma$  neutralizing antibodies ameliorates UC by decreasing VP. Qingchang suppository, which has been used in treating rectitis and colitis in Shanghai, China, decreases VP in DSS-induced colitis.<sup>4</sup> As a key cytokine that increases VP, serum vascular endothelial growth factor (VEGF) level is increased in UC patients,<sup>7</sup> and blockade of VEGF signaling pathway reduces severity of experimental UC in rats.<sup>8,9</sup> However, other factors that contribute to increased VP in colitis remain largely unexplored.

Fibrinogen (Fg) is a soluble 340-kDa glycoprotein and is composed of 3 distinct polypeptide chains called A $\alpha$ , B $\beta$ , and  $\gamma$ , which are encoded by 3 separate genes Fga, Fgb, and Fgg, respectively.<sup>10</sup> The 3 chains make an elongated molecule and form the homodimeric Fg molecule that circulates in the blood.<sup>10</sup> As the end product of coagulation cascade, Fg has been shown to modulate inflammation in several pathological conditions. Cleavage of Fg by proteinases elicits allergic responses through activating Toll-like receptor 4 as a ligand.<sup>11</sup> In the central nervous system, Fg promotes autoimmunity and demyelination via chemokine release and antigen presentation.<sup>12</sup> In addition, Fg promotes inflammation by activating monocytes via CD11b/CD18 receptors. More importantly, Fib $\gamma$ <sup>390-396A</sup> mice, which lack the leukocyte integrin receptor  $\alpha_M\beta_2$  binding motif, are less susceptible to azoxymethane/DSS-induced colitis and colitis-associated cancer.<sup>13</sup> However, the effect of Fg on VP in colitis remains unknown.

Based on our previous high-throughput proteomic analysis,<sup>14</sup> we found significant upregulation of Fg in colons of DSS-treated mice. Moreover, the pathological symptoms and motility of DSS-treated mice were ameliorated by inhibition of Fg polymerization. Mechanism investigation suggests that Fg promotes VP by activating AKT and

subsequent microfilament depolymerization. Our study raises the possibility of Fg as a potential therapeutic target for anti-colitis treatment.

## Results

### *Fg Is Upregulated in Colons of DSS-Treated Mice and UC Patients*

To identify vital proteins that are dysregulated in the inflamed colon, we utilized a DSS-induced colitis mouse model for quantitative proteomics.<sup>14</sup> Control mice were given drinking water for 10 days while DSS-treated mice were given 3% DSS for 7 days that was replaced with drinking water for the following 3 days. Compared with the drinking water-treated control mice, protein levels of 3 Fg subunits (Fib $\alpha$ , Fib $\beta$ , and Fib $\gamma$ ) were significantly increased in the colons of DSS-treated mice (Figure 1A).<sup>14</sup> In addition, the upregulation of Fg in the colons of DSS-treated mice was confirmed by immunoblotting and immunohistochemical staining (Figure 1B and C). Increased Fg level was also observed in UC patients by immunofluorescence staining (Figure 1D). These data show that the protein level of Fg was significantly increased in colitis.

### *Pharmacological Inhibition of Fibrinogen Ameliorates DSS-Induced Colitis*

To determine the role of Fg in DSS-induced colitis, Gly-Pro-Arg-Pro acetate (GPRP) was used to inhibit the interaction of Fg with its receptors in vivo.<sup>15-18</sup> In the DSS-induced colitis mouse model, GPRP was given daily by intraperitoneal injection. Compared with the control treatment (distilled water), GPRP significantly inhibited body weight loss and dramatically reduced DSS-induced mortality and shortening of colon length (Figure 2A-C). Hematoxylin and eosin staining showed that GPRP significantly decreased disease severity, colon damage, and cell death in DSS-treated mice (Figure 2D-G). Next, we examined whether GPRP decreased inflammation in DSS-induced colitis. Hematoxylin and eosin staining showed that GPRP significantly decreased tissue damage and infiltration of inflammatory cells in colons of DSS-treated mice (Figure 2E). Enhanced tissue damage in water-treated mice was accompanied with augmented expression of proinflammatory cytokines and chemokines, including tumor necrosis factor alpha (TNF- $\alpha$ ), interleukin (IL)-1 $\beta$ , IL-17A, GM-CSF (granulocyte-

\*Authors share co-first authorship.

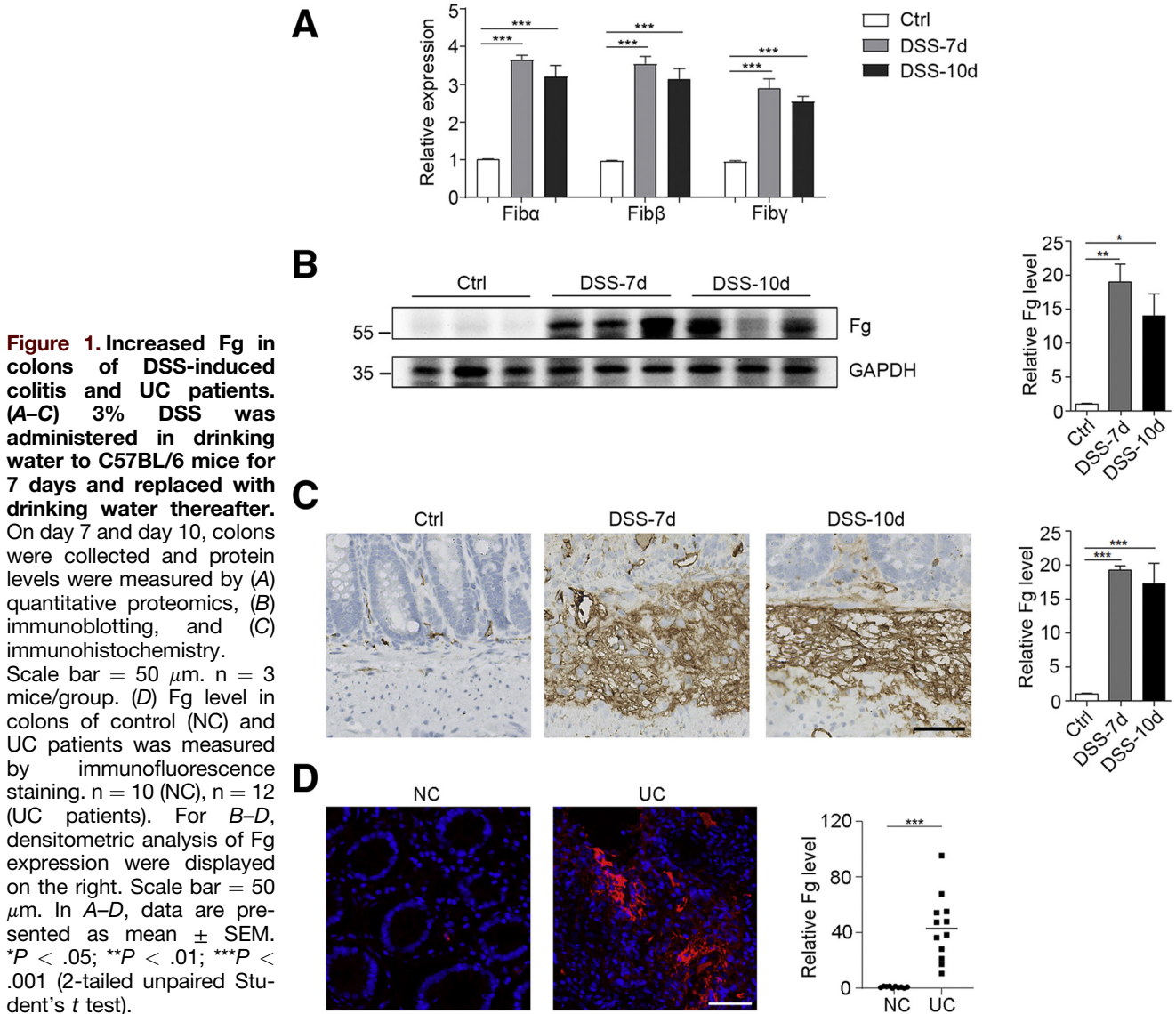
**Abbreviations used in this paper:** DSS, dextran sulfate sodium; eNOS, endothelial nitric oxide synthase; Fg, fibrinogen; GPRP, Gly-Pro-Arg-Pro acetate; IBD, inflammatory bowel disease; IFN- $\gamma$ , interferon gamma; IL, interleukin; p-AKT, phosphorylated AKT; TNF- $\alpha$ , tumor necrosis factor alpha; TNBS, trinitrobenzene sulfonic acid; TUNEL, terminal deoxynucleotidyl transferase-mediated deoxyuridine triphosphate nick-end labeling; UC, ulcerative colitis; VEGF, vascular endothelial growth factor; VP, vascular permeability.

 Most current article

© 2020 The Authors. Published by Elsevier Inc. on behalf of the AGA Institute. This is an open access article under the CC BY-NC-ND license (<http://creativecommons.org/licenses/by-nc-nd/4.0/>).

2352-345X

<https://doi.org/10.1016/j.jcmgh.2020.10.007>



macrophage colony-stimulating factor), IL-6, LIX (lipopolysaccharide-induced CXC chemokine), KC (keratinocytes-derived chemokine), MCP-1 (monocyte chemoattractant protein-1), and MIP-2 (macrophage inflammatory protein-2), which were significantly restrained in GPRP-treated mice (Figure 3A–C). However, the levels of Th1 cytokines (IFN- $\gamma$ , IL-12) and Th2 cytokines (IL-4, IL-5, IL-7, IL-10, IL-13) were not significantly changed between control and DSS-treated mice (Figure 3D). In DSS-induced colitis, large numbers of myeloid cells (CD11b positive), macrophages (F4/80 positive), and neutrophils (MPO positive) infiltrated into the mucosa and epithelial layer of the damaged colon (Figure 4A–C). The infiltration of CD11b-, F4/80-, and MPO-positive cells in the colon was dramatically suppressed in GPRP-treated mice (Figure 4A–C). The same phenomenon was also observed with the infiltration of S100A9-positive cells, a marker of inflammation (Figure 4D). Taken together, these results imply that inhibition of Fg signaling

ameliorates DSS-induced colitis in mice, suggesting that upregulation of Fg contributes to the progression of DSS-induced colitis.

### GPRP Decreases Intestinal Vascular Permeability in Colons of DSS-Treated Mice

Increased VP is required for the infiltration of inflammatory cells into the tissue; thus, we explored whether GPRP attenuated colonic VP in DSS-treated mice. As expected, extravasation of serum albumin, indicated by the content of Evans blue, was significantly increased in colons of DSS-treated mice (Figure 5A and B), suggesting an increase of colonic VP in DSS-treated mice. Moreover, GPRP significantly decreased colonic VP in DSS-treated mice (Figure 5A and B).

To confirm whether Fg directly increased VP, we adopted the model of skin VP. As expected, Fg alone induced

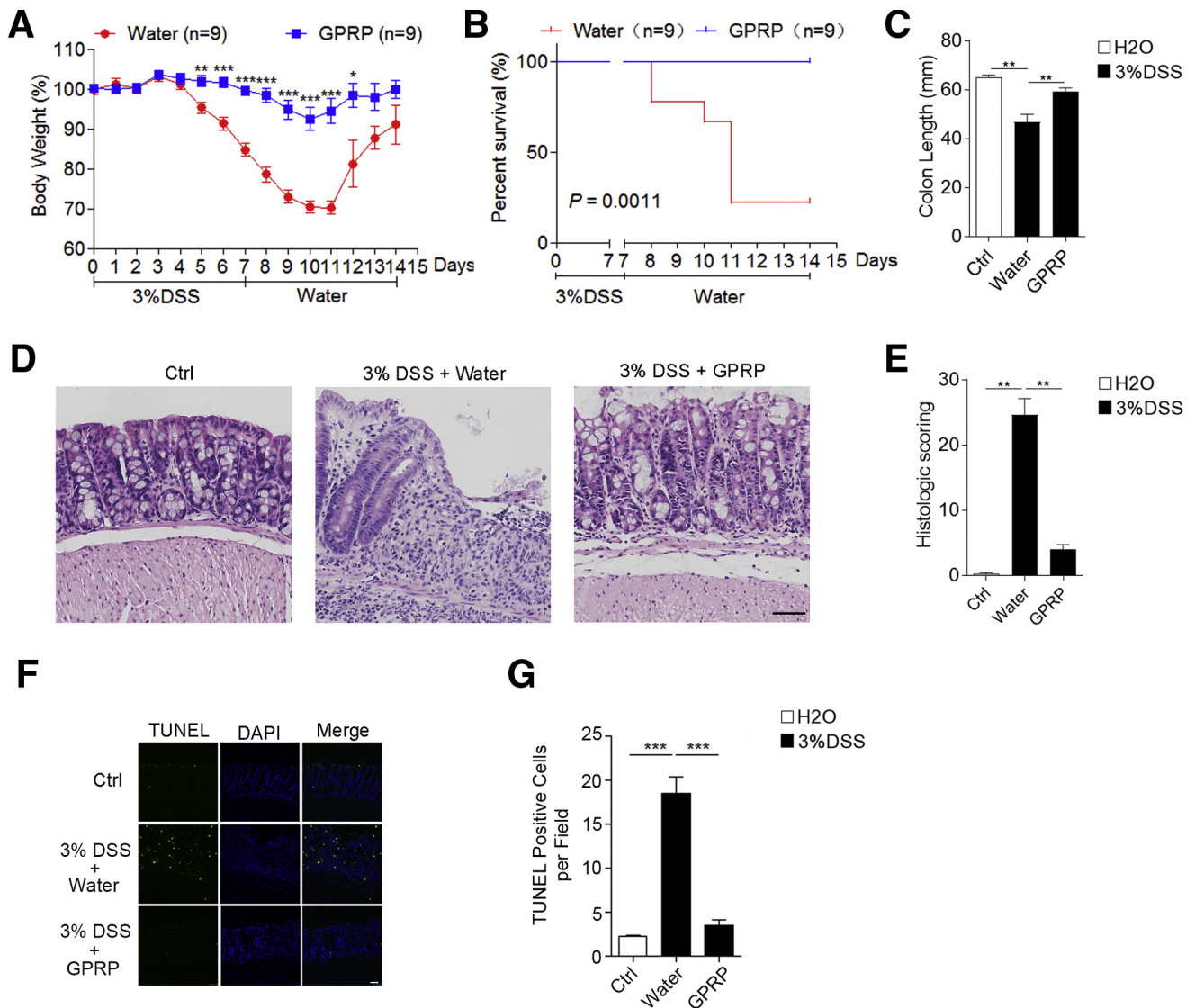


**Figure 2. GPRP ameliorated DSS-induced colitis in vivo; 3% DSS was administered in drinking water to C57BL/6 mice for 7 days and replaced with fresh water thereafter.** GPRP (100 mg/kg) or distilled water was injected intraperitoneally every day for 10 days. (A) Body weight and (B) survival rate was determined;  $n = 9$  mice/group. (C) Mice were sacrificed on day 7 to measure the colon length; colon tissues from mice on day 7 were evaluated by (D) hematoxylin and eosin staining and (E) histologic scoring analysis, or (F, G) TUNEL staining;  $n = 4$  mice/group. Scale bar = 50  $\mu\text{m}$ . In A, C, E, and G, data are presented as mean  $\pm$  SEM. \* $P < .05$ ; \*\* $P < .01$ ; \*\*\* $P < .001$  (2-tailed unpaired Student's  $t$  test).

strong vascular leakage in skin, as indicated by Miles permeability assay (Figure 5C). Furthermore, GPRP inhibited Fg-induced VP (Figure 5D). These data suggest that Fg may promote DSS-induced colitis by enhancing colonic VP and facilitating the infiltration of inflammatory cells.

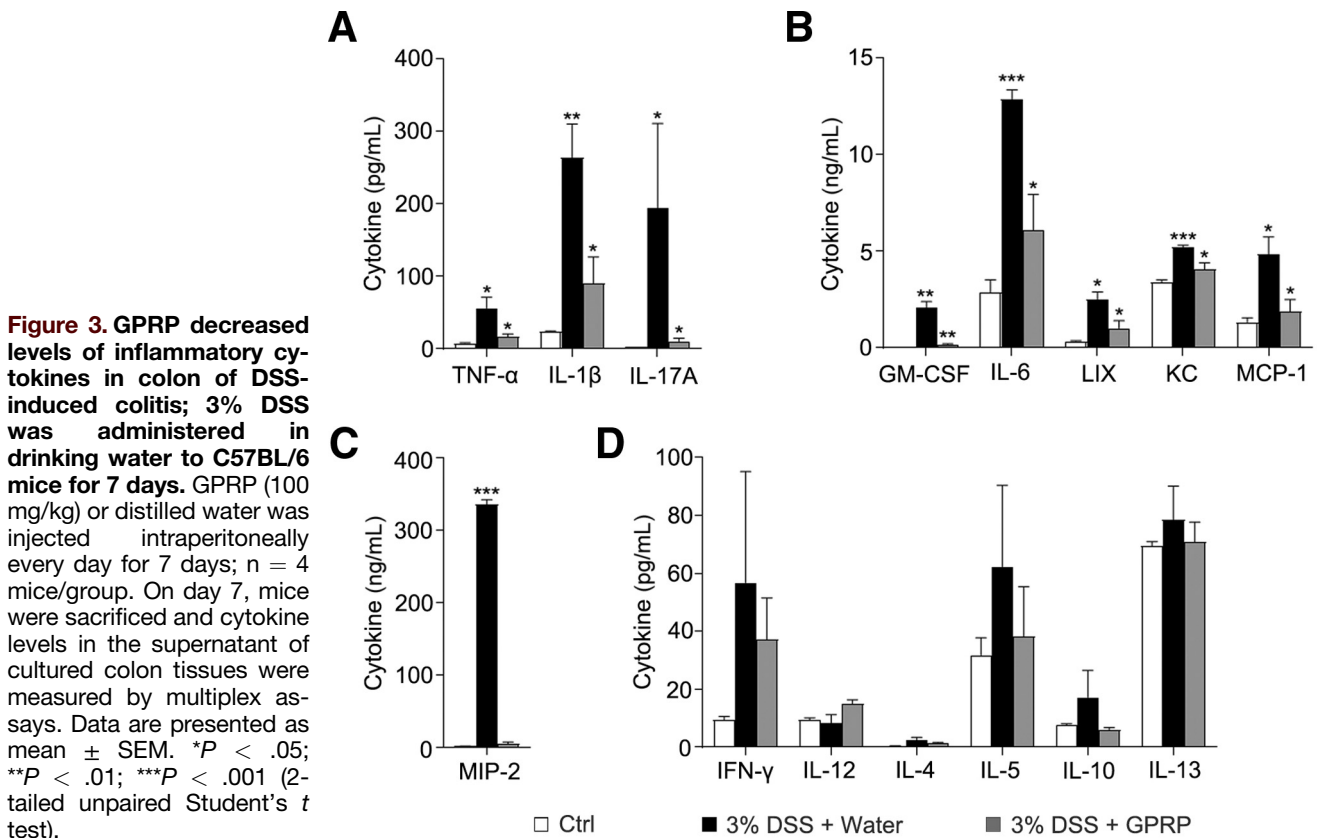
#### Fg Promotes Cell-to-Cell Disaggregation In Vitro

To explore the role of Fg in vitro, we directly used Fg to stimulate mouse endothelial cell MS1. A video time-lapse analysis showed that after Fg stimulation, the cell-to-cell attachment dramatically decreased (Figure 6A), and this kind of disaggregation was not because of cell death (Figure 6B). Confocal fluorescence microscopy revealed that Fg decreased distribution of microfilaments at the cell

junction (Figure 6C). Furthermore, monomer/polymer-actin ratio in cells was increased after Fg stimulation (Figure 6D and E). Taken together, Fg could induce microfilament depolymerization and finally promote cell-to-cell disaggregation in vitro.

#### Fg Disrupts Vascular Barrier by Inducing AKT Activation and Subsequent Depolymerization of Microfilament

Activation of FAK (focal adhesion kinase)/SRC (SRC proto-oncogene, nonreceptor tyrosine kinase) and AKT are different mechanisms for the induction of VP. Then we examined which signaling pathway was essential for Fg-induced VP. FAK inhibitors (defactinib and Y15) or SRC



inhibitors (saracatinib and WH-4-023) had no effect on Fg-induced VP (Figure 7A–C), while PI3K inhibitors (LY294002 and tasisib) slightly decreased and AKT inhibitors (caviasertib and MK 2206) blocked Fg-induced VP (Figure 7D–F), suggesting activation of AKT was responsible for Fg-induced VP.

Activation of endothelial nitric oxide synthase (eNOS) has been shown to be the downstream target of AKT to induce VP in vitro. However, eNOS inhibitor (L-NIO and L-NMMA) did not decrease Fg-induced VP in vivo (Figure 8A and C), suggesting that other mechanism was responsible for Fg/Akt-induced VP. Previous reports showed that cytoskeleton was involved in regulating VP, so we explored whether polymerization and depolymerization of microfilaments or microtubules were involved in Fg-induced VP. However, microtubule stabilizers (docetaxel and epothilone B) had no effect on Fg-induced VP (Figure 8B and C). Interestingly, low doses of Jasplakinolide (actin polymerization inducer) attenuated Fg-induced VP, while both high doses of Jasplakinolide and Cytochalasin D (an inhibitor of actin polymerization) dramatically increased Fg-induced VP (Figure 8D–G). These results suggest that the maintenance of vascular barrier mainly depends on the status of microfilaments. Interfering the balance between polymerization and depolymerization of microfilaments could finally affect the VP.

To directly explore the role of Fg on AKT activation, we stimulated mouse endothelial cell MS1 with Fg in vitro. As

expected, Fg induced strong AKT activation, as indicated by induction of AKT phosphorylation (Figure 9A). As showed in Figure 6D, Fg could increase monomer/polymer-actin ratio, but this phenomenon was restrained by AKT inhibitor (Figure 9B).

Next, we examined whether AKT was activated in DSS-induced colitis. As expected, phosphorylated AKT (p-AKT) was significantly increased in colons of DSS-treated mice (Figure 9C), suggesting activation of AKT in DSS-induced colitis. Consistently, Fg deposits and phosphorylation of AKT were also increased in trinitrobenzene sulfonic acid (TNBS)-induced colitis (Figure 9D–F). To confirm the activation of AKT in colonic vessels in DSS-induced colitis, we co-stained p-AKT with a vascular marker (CD31). Colocalization of p-AKT and CD31 was observed in colons of DSS-treated mice instead of control mice (Figure 9G), suggesting activation of AKT in colonic vessels of DSS-treated mice.

Collectively, these data suggest that Fg promoted AKT activation and subsequent microfilament depolymerization, all of which play an important role in the induction of VP in colitis.

## Discussion

In this article, we revealed that Fg was increased in the colons of DSS/TNBS-induced colitis and UC patients; it enhanced VP by activating AKT and subsequent

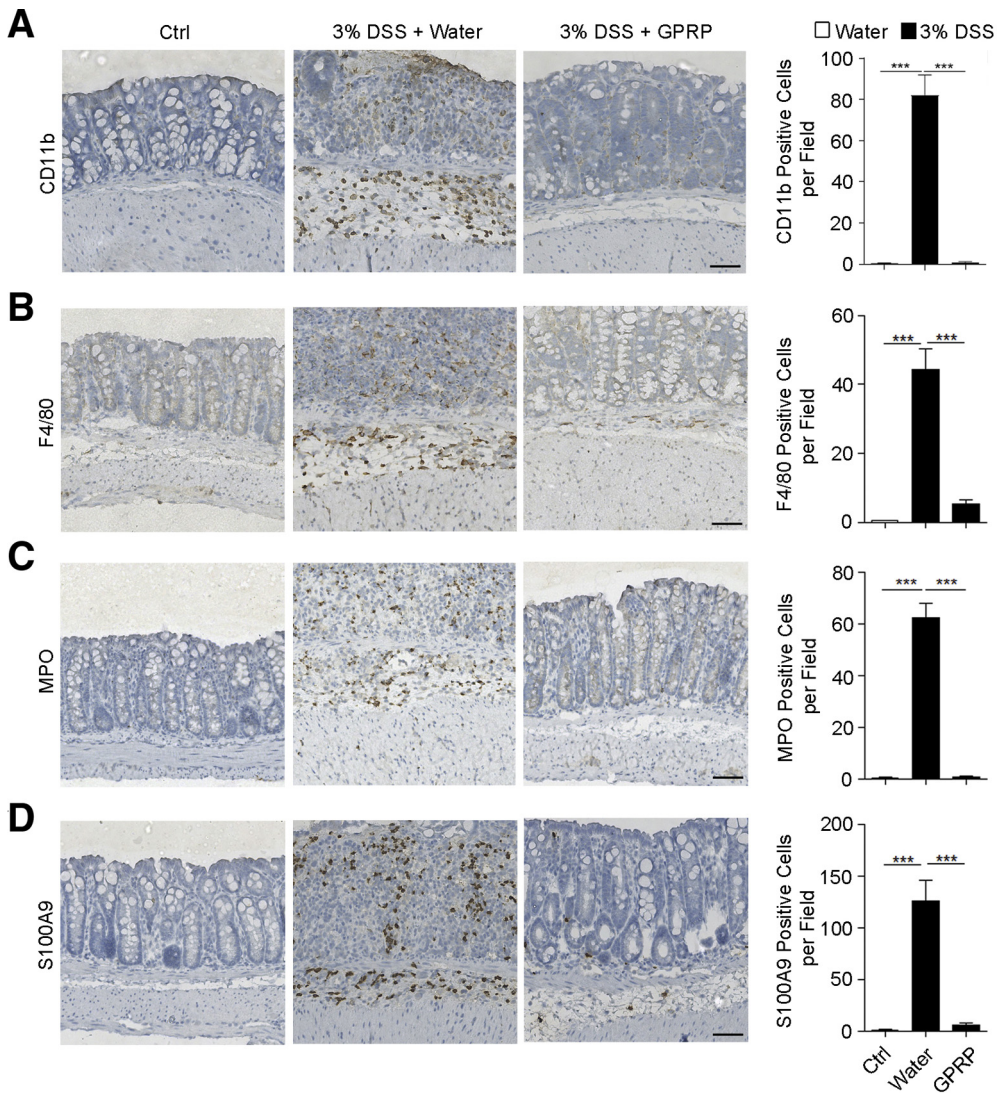


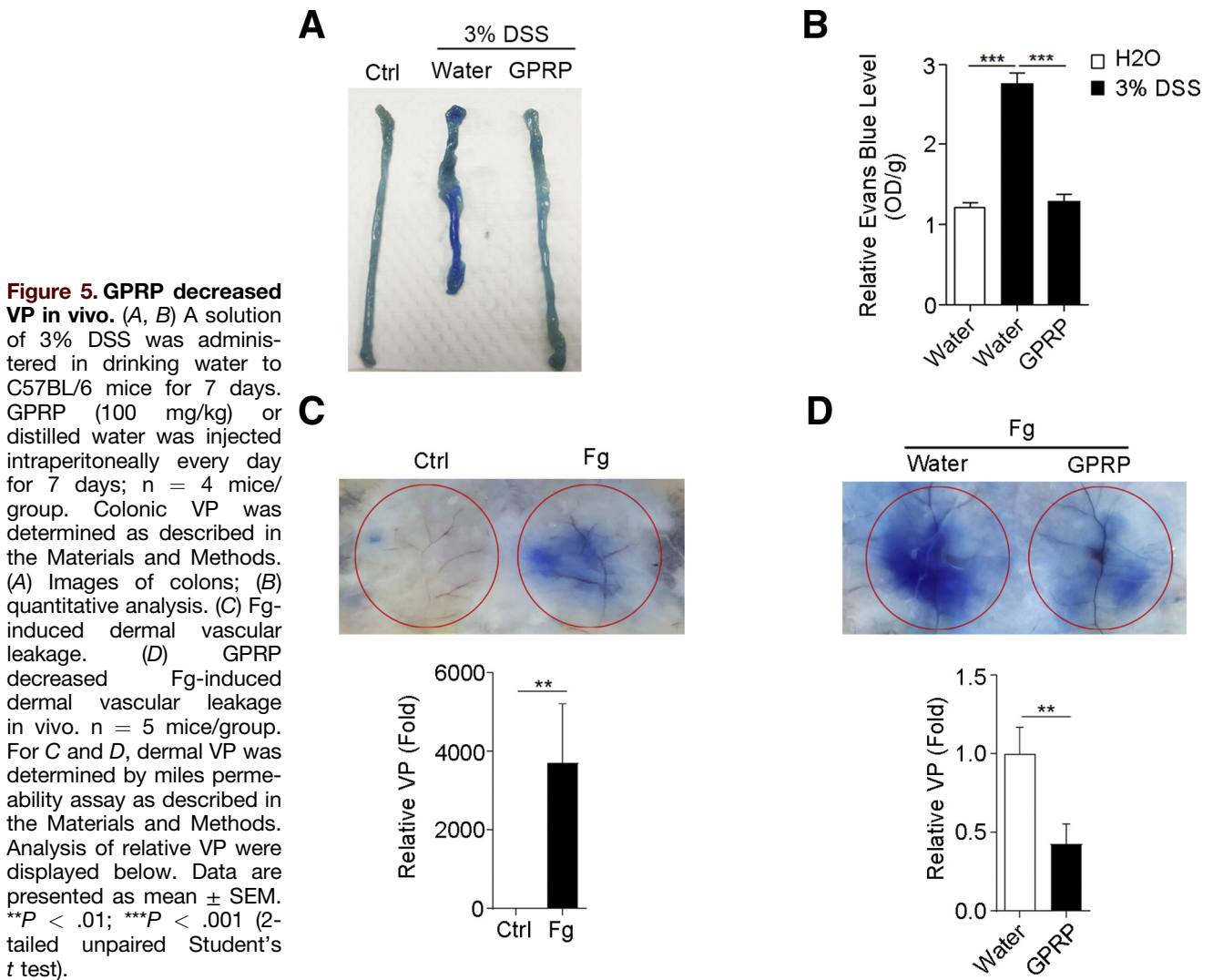
**Figure 4.** GPRP decreased the infiltration of CD11b-, F4/80-, MPO-, and S100A9-positive cells in colons of DSS-treated mice. (A–D) A solution of 3% DSS was administered in drinking water to C57BL/6 mice for 7 days. GPRP (100 mg/kg) or distilled water was injected intraperitoneally every day for 7 days,  $n = 4$  mice/group. Colons were harvested and sections of colon tissues were immunohistochemically stained for (A) CD11b, (B) F4/80, (C) MPO, and (D) S100A9 with corresponding antibodies. Scale bar = 50  $\mu\text{m}$ . Ten random fields (200 $\times$ ) were photographed for each section. The average number of positive cells per field is presented. In A–D, data are presented as mean  $\pm$  SEM. \*\*\* $P < .001$  (2-tailed unpaired Student's  $t$  test).

microfilament depolymerization. Inhibiting Fg polymerization by GPRP treatment ameliorated VP and DSS-induced colitis in vivo. Our findings suggest that targeting Fg may be a potential therapy for colitis.

VP is a complex process that is regulated by several cytokines and plays important roles in inflammation-related disease, including IBD. Targeting VP has been indicated to serve as a new therapy for inflammation-associated disorders. Anti-TNF therapy is clinically used for IBD treatment.<sup>19</sup> Except for promoting inflammation and cell death, TNF- $\alpha$  is also an inducer of VP.<sup>20,21</sup> Therefore, decreasing VP may be another reason for the effectiveness of anti-TNF therapy for IBD. In this article, we found that Fg was significantly increased in colons of DSS-induced colitis and dramatically increased VP in vivo for the first time. GPRP ameliorated DSS-induced colitis, as indicated by decreased secretion of proinflammatory cytokines, infiltration of inflammatory cells, colon length shortening, body weight loss, and mortality. These results

suggest targeting VP by Fg inhibition may serve as a new therapy for colitis.

The interaction of thrombin and Fg increased VP in lung injury.<sup>22</sup> ICAM1 (intercellular adhesion molecule 1)/ERK (extracellular regulated kinase) and integrin/RhoA were found to be involved in Fg-induced leakage of endothelial cell monolayer.<sup>22</sup> Based on our data, Fg-enhanced VP in vivo is dependent on AKT activation. VEGF is the most widely studied cytokine that increases VP, and FAK/SRC signaling is vital for VEGF-induced VP.<sup>23–25</sup> However, neither FAK inhibitors nor SRC inhibitors decreased Fg-induced VP in vivo, suggesting that Fg enhanced VP independently of FAK/SRC signaling pathway. Although less well studied, AKT can also regulate VP by promoting nitric oxide production.<sup>26,27</sup> Meanwhile, AKT inhibitors nearly blocked Fg-induced VP in vivo. Moreover, activation of AKT was observed in colonic vessels in DSS/TNBS-induced colitis and Fg directly induced activation of AKT in vitro. These results suggest AKT activation is vital to Fg-induced VP. However,



inhibition of PI3K, upstream of AKT, was not as efficient as inhibition of AKT in blocking Fg-induced VP, suggesting that other upstream regulators of AKT are involved in Fg-induced AKT activation. Endothelium-derived nitric oxide is another important promoter of VP and is produced by eNOS.<sup>28,29</sup> Phosphorylation of eNOS by AKT is required for efficient production of nitric oxide.<sup>26</sup> However, eNOS inhibitors had no effect on Fg-induced VP, suggesting that Fg/AKT-induced VP is independent of eNOS pathway.

Cell-cell and cell-matrix adhesions are essential for barrier maintenance and restoration.<sup>30</sup> The cytoskeleton is a key regulator in maintaining endothelial integrity and in restoring integrity following injurious denudation.<sup>31</sup> Disruption and dysfunction of the cytoskeleton may result in impairment of endothelial function, subsequently tipping the balance toward vascular disease.<sup>31</sup> Previous studies suggested that microfilaments and microtubules are involved in the regulation of VP.<sup>32</sup> In our study, we found

that microtubule stabilizers (docetaxel and epothilone B) had no effect on Fg-induced VP, suggesting that microtubule was not involved in Fg-induced VP. Interestingly, low doses of Jasplakinolide attenuated Fg-induced VP, while both inhibitors of actin polymerization (Cytochalasin D) and high doses of Jasplakinolide dramatically increased Fg-induced VP. It is worth noting that low doses of Jasplakinolide stabilized actin filaments in vitro, but high doses of Jasplakinolide increased permeability (hydraulic conductivity) to the same extent as Cytochalasin D, interrupted the junction-associated actin filament system, and induced formation of intercellular gaps in cultured myocardial endothelial cell monolayers.<sup>33</sup> Intercellular contacts along the endothelial monolayer are linked to the actin cytoskeleton to provide mechanical stability of endothelial cells.<sup>30</sup> Therefore, the stability of microfilaments' structure is essential to maintain vascular barrier. Together, these results suggest that Fg may induce VP by promoting microfilament depolymerization.

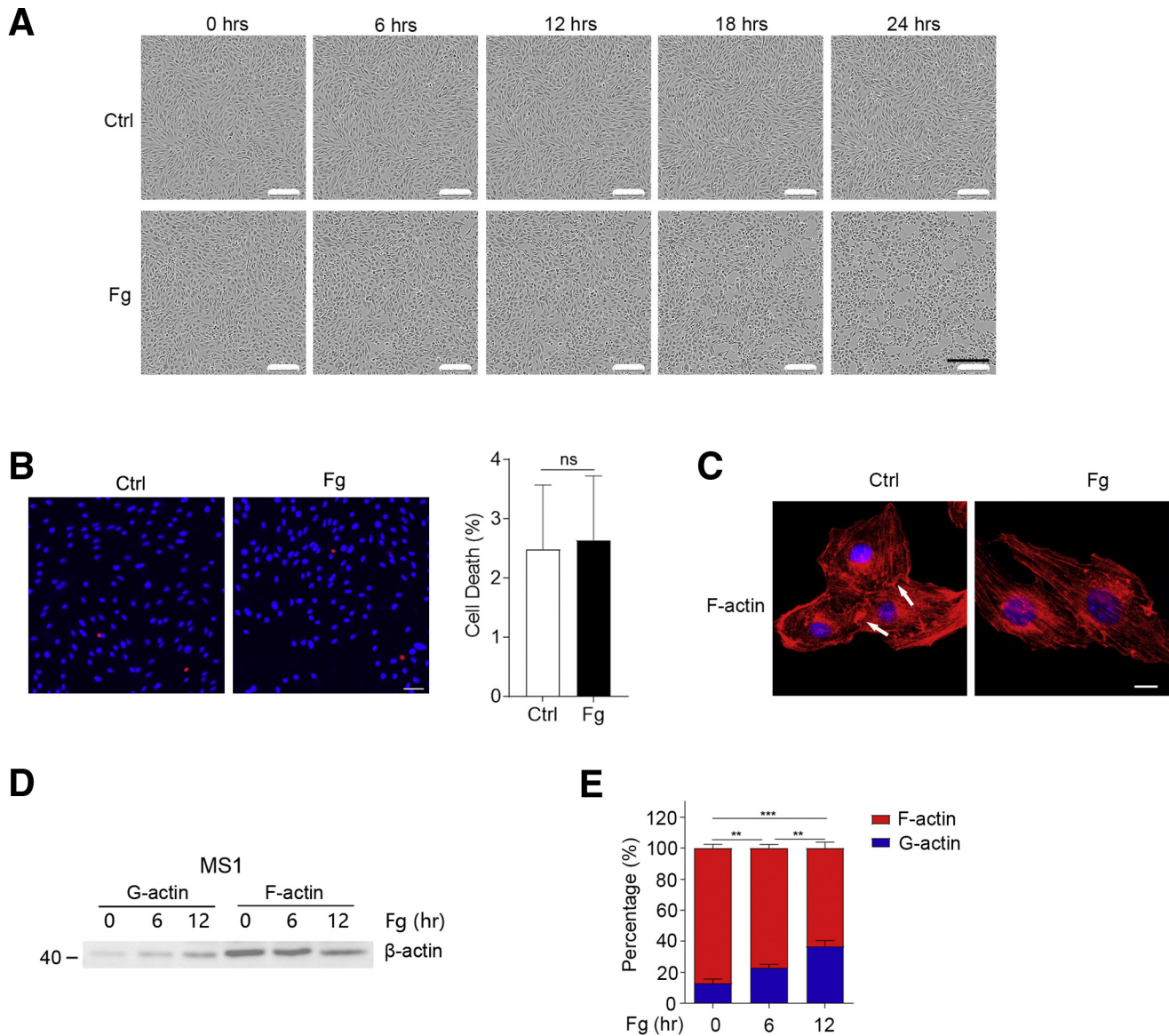


**Figure 6. Fg promotes cell-to-cell disaggregation in vitro.** (A, B) MS1 cells were stimulated with or without Fg (5 mg/mL) for (A) indicated times or (B) 24 hours. (A) Cells were photographed by time lapse. Scale bar = 300  $\mu$ m. (B) Cell death was analyzed by PI/Hoechst staining; cell death (%) = (PI positive cells / Hoechst positive cells)  $\times$  100%. Scale bar = 50  $\mu$ m. (C) Fg decreased distribution of microfilaments at the cell junction. MS1 cells were stimulated with or without Fg for 12 hours and stained with phalloidin. Scale bar = 10  $\mu$ m. (D, E) Fg induced microfilament depolymerization in MS1 cells. MS1 cells were stimulated with Fg (5 mg/mL) for indicated times, (D) G-actin and F-actin were detected by fractionation and immunoblotting, and (E) densitometric analysis of actin level by the ImageJ program. In B and E, data are presented as mean  $\pm$  SEM. \*\* $P$  < .01; \*\*\* $P$  < .001; ns,  $P$  > .05 (2-tailed unpaired Student's  $t$  test).

Previous studies found that Akt regulated actin organization and cell motility.<sup>34,35</sup> Herein, we observed that Fg induced activation of AKT and subsequent microfilament depolymerization in vitro in a time-dependent manner, suggesting that AKT activation is upstream of microfilament depolymerization. Moreover, inhibition of AKT decreased Fg-induced microfilament depolymerization. Together with the in vivo results, we speculate that Fg increases VP by induction of AKT activation and subsequent microfilament depolymerization.

Taken together, our data imply a key role of Fg/AKT/microfilament depolymerization in promoting

pathogenesis of DSS-induced colitis by enhancing VP and suggest Fg as a potential target for colitis treatment.

## Materials And Methods

### Cell Lines

Mouse pancreatic islet endothelial cell MS1 was maintained in Dulbecco's modified Eagle's medium (Gibco Laboratories, Gaithersburg, MD) supplemented with 10% fetal bovine serum, penicillin (100 U/mL), and streptomycin (100 U/mL).

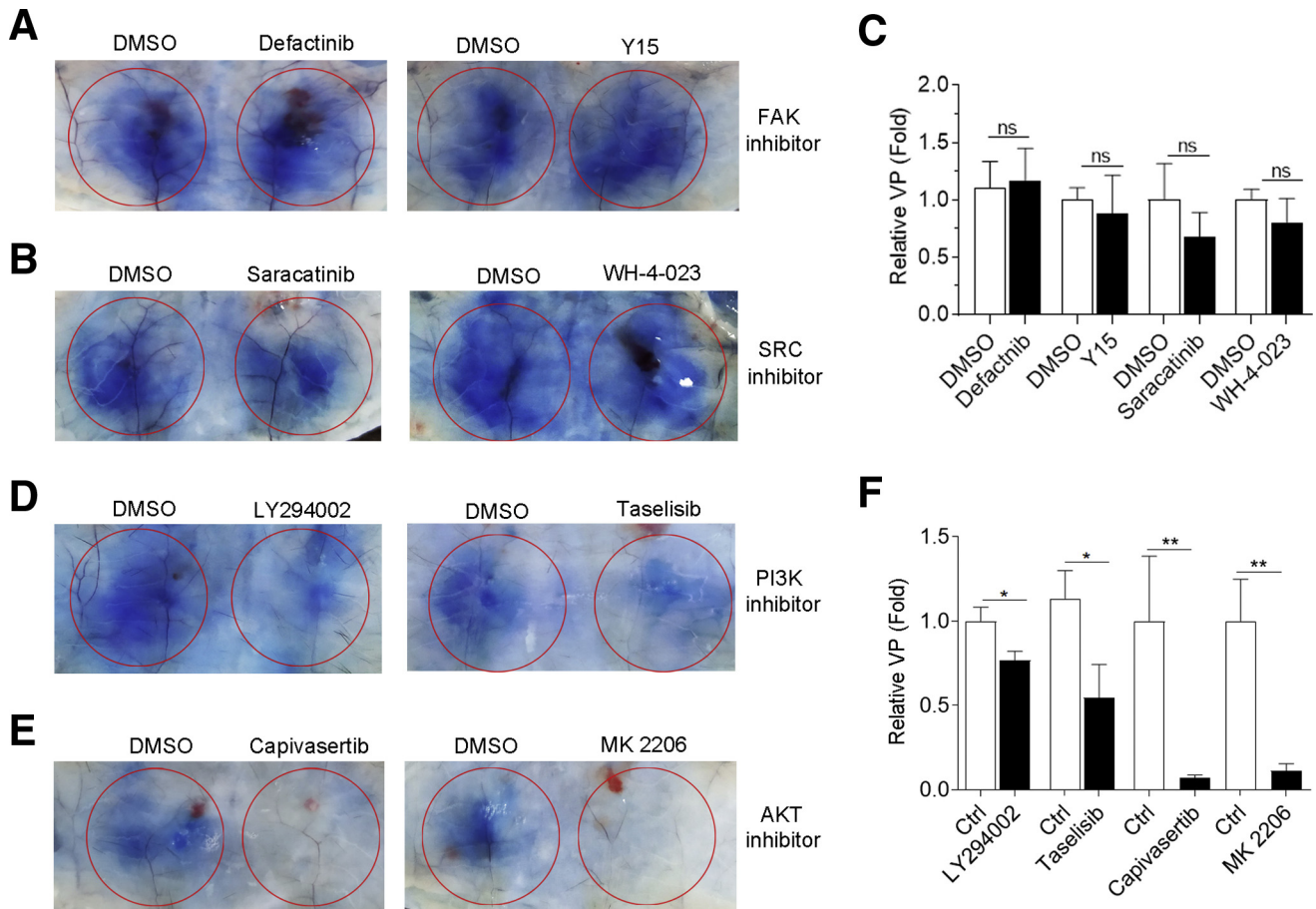


**Figure 7.** The effect of FAK/SRC inhibitors and PI3K/AKT inhibitors on Fg-induced VP. Fg supplemented with dimethyl sulfoxide (DMSO) or indicated inhibitors were injected beneath abdominal dermis of mice. One hour later, mice were injected intravenously with Evans blue. (A, B, D, E) Thirty minutes later, VP was examined. (C, F) Densitometric analysis of relative VP.  $n = 5-7$  mice/group. \* $P < .05$ ; \*\* $P < .01$ ; ns,  $P > .05$  (2-tailed unpaired Student  $t$  test).

### Patients and Specimens

Twelve patients with active UC and 10 healthy control subjects were enrolled at the Second Affiliated Hospital of Guangzhou Medical University (Guangzhou, China). People with functional gastrointestinal disorders and normal endoscopy and histology served as control subjects. Mucosal biopsy specimens were taken from colonic districts. The samples have been obtained according the regulations and after approval of an institutional review board protocol of the Second Affiliated Hospital of Guangzhou Medical University.

### Reagents

The antibodies used for immunoblotting included: mouse monoclonal antibody against GAPDH (RM2002; Beijing Ray, Beijing, China); rabbit antibodies against Fg (ab189490; Abcam, Cambridge, MA), pan-Akt (4691; Cell Signaling Technology, Danvers, MA), p-Akt (Ser473) (4060; Cell Signaling Technology), and goat anti-mouse (R3001, Beijing Ray) or goat anti-rabbit (R3002, Beijing Ray) horseradish peroxidase-conjugated secondary antibody.

The antibodies used for immunohistochemical staining included: CD11b (ab133357; Abcam), S100A9 (73425; Cell

Signaling Technology), MPO (ab9535; Abcam), F4/80 (ab111101; Abcam), and CD31 (3528; Cell Signaling Technology).

Other reagents included DSS (36,000–50,000 kD; MP Biomedicals, Santa Ana, CA), Evans blue (E2129; Sigma-Aldrich, St. Louis, MO), Fg (F3879; Sigma-Aldrich), GPRP acetate, LY294002, tselisib, capivasertib, MK 2206, defactinib, Y15, saracatinib, WH-4-023, L-NIO, L-NMMA, ML-7, MLCK inhibitor, docetaxel, Jaspilkinolide, and Cytochalasin D (MedChemExpress, Monmouth Junction, NJ).

### DSS-Induced Colitis Model

Male C57BL/6 mice weighing 21–23 g were housed in specific pathogen-free facility at the Second Affiliated Hospital of Guangzhou Medical University. Control mice were given drinking water for 10 days. For DSS-induced colitis, DSS (3% wt/vol) was administered in drinking water ad libitum for 7 days (from day 0 to day 7). DSS solution was replaced twice on day 2 and day 4, and the beddings were not changed during the whole experiments. For GPRP acetate intervention experiments, mice were injected intraperitoneally with GPRP (100 mg/kg, dissolved in distilled water) or distilled water daily. Mice weight and survival

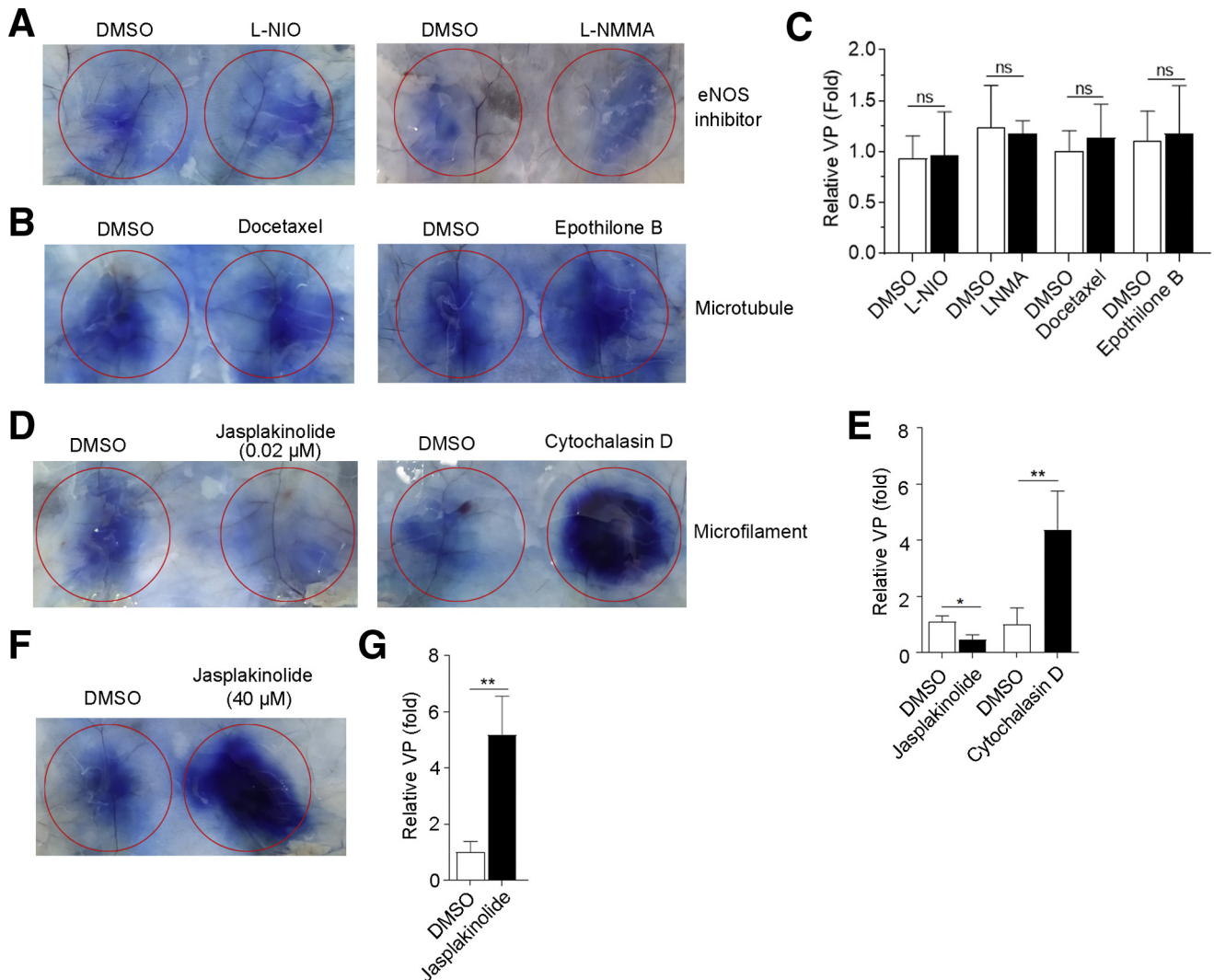


**Figure 8.** The effect of eNOS inhibitors, microtubule stabilizers, and inducer and inhibitor of microfilaments on Fg-induced VP. Fg supplemented with DMSO or indicated inhibitors were injected beneath abdominal dermis of mice. One hour later, mice were injected intravenously with Evans blue. (A, B, D, F) Thirty minutes later, VP was examined. (C, E, G) Densitometric analysis of relative VP.  $n = 5-7$  mice/group. \* $P < .05$ ; \*\* $P < .01$ ; ns,  $P > .05$  (2-tailed unpaired Student  $t$  test).

were recorded daily for 12 days. For colon length, hematoxylin and eosin, terminal deoxynucleotidyl transferase-mediated deoxyuridine triphosphate nick-end labeling (TUNEL) and immunoblotting, the experiments lasted for 7 days. Histologic scoring was conducted as previously described.<sup>14</sup> All protocols involving animals were conducted in accordance with the Guide for the Care and Use of Laboratory Animals (National Institutes of Health publication Nos. 80-23, revised 1996) and under the approval of the Ethical Committee of Guangdong Provincial Animal Experiment Center.

### Immunoblotting

Tissue or cell proteins were separated in polyacrylamide gels and transferred to methanol activated polyvinylidene difluoride membranes. The membranes were blocked for 1 hour in Tris-buffered saline plus Tween-20 containing 3%

bovine serum albumin or 5% milk, and then immunoblotted sequentially with primary and secondary antibodies. The protein levels were detected using a Pierce ECL Western blotting substrate (Thermo Fisher Scientific, Waltham, MA).

### Immunohistochemical and Immunofluorescent Staining

Sections of paraformaldehyde-fixed, paraffin-embedded tissues were deparaffinized with xylene and rehydrated through graded ethanol, followed by quenching of endogenous peroxidase activity in 0.3% hydrogen peroxide and antigen retrieval by microwave heating in 10-mM citrate buffer (pH 6.0) for Fg, Cd11b, S100A9, Cd31, and p-Akt, or in EDTA buffer (pH 9.0) for MPO and F4/80. Sections were incubated at 4°C overnight with rabbit polyclonal antibody against Fg, S100A9, MPO, and F4/80, then immunostained

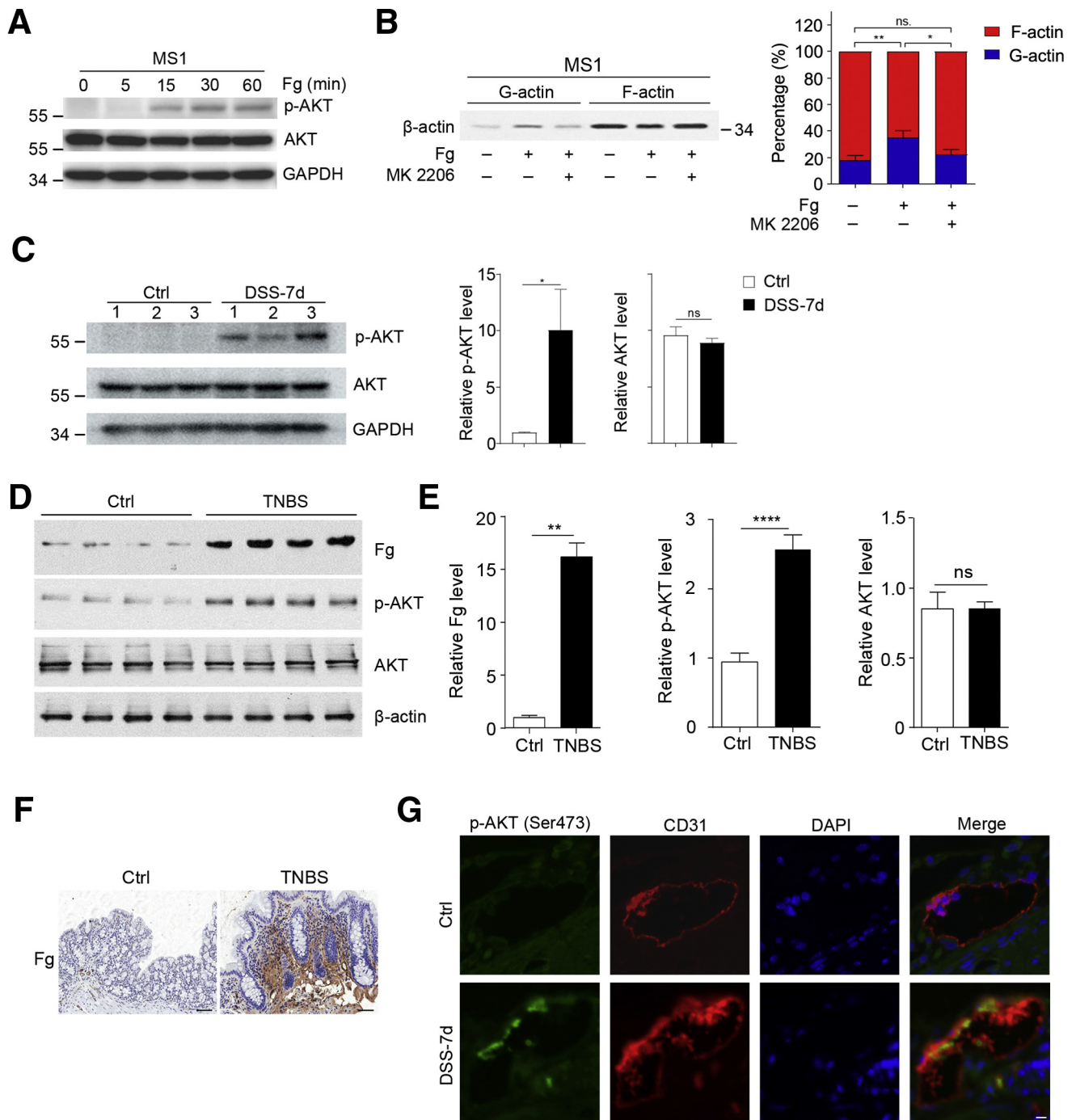


**Figure 9. Activation of AKT in Fg-treated endothelial cells and colonic vessels of DSS-treated mice.** (A) Fg induced AKT activation in MS1 cells. MS1 cells were stimulated with Fg (5 mg/mL) for indicated times, then proteins were immunoblotted with indicated antibodies. GAPDH was served as an internal control. (B) AKT inhibitor decreased Fg-induced microfilament depolymerization. MS1 cells were treated with Fg supplemented with DMSO or MK 2206 for 12 hours, then G-actin and F-actin were detected by fractionation and immunoblotting, and densitometric analysis of actin level by the ImageJ program is displayed on the right. (C) p-AKT (Ser473) was increased in colons of DSS-treated mice. Distilled water or 3% DSS was administered in drinking water to C57BL/6 mice for 7 days. Colonic proteins on day 7 were tested by immunoblotting to detect p-AKT (473), and AKT with corresponding antibodies. GAPDH was used as an internal control.  $n = 3$  mice/group. (D–F) Increased Fg and p-AKT in TNBS-induced colitis. For experimental colitis, 150-mg/kg TNBS dissolved in ethanol was used to treat BalB/C mice through rectum. On day 4, colon tissues were harvested for (D, E) immunoblotting and (F) immunohistochemical analysis. (G) Colocalization of p-AKT and colonic vessels in DSS-treated mice. Colonic sections of control and DSS-treated mice were double immunofluorescence stained with anti-p-AKT (Ser473) and anti-CD31 (marker of vessels). Scale bar = 10  $\mu\text{m}$ . \* $P < .05$ ; \*\* $P < .01$ ; \*\*\*\* $P < .0001$ ; ns,  $P > .05$  (2-tailed unpaired Student  $t$  test).

by ChemMate DAKO EnVision Detection Kit, Peroxidase/DAB, Rabbit/Mouse (DakoCytomation, Glostrup, Denmark). Subsequently, sections were counterstained with hematoxylin and mounted in nonaqueous mounting medium. For immunofluorescent staining, sections were stained with anti-rabbit IgG (H+L), F(ab')<sub>2</sub> Fragment (Alexa Fluor 555 Conjugate; Thermo Fisher Scientific) after primary antibody incubation. For double immunofluorescent staining, 2 rounds of tyramide signal amplification were performed for detection of CD31 and p-AKT.

To evaluate protein levels, 5 representative staining fields (200×) were examined for each section. The protein levels of Fg were estimated by density scanning using ImagePro Plus software (Media Cybernetics, Silver Spring, MD). To detect the number of CD11b, S100A9, MPO or F4/80 positive cells, 10 representative fields (200×) were photographed for each section and the average numbers of cells per field were presented.

### Detection of Cytokines

Colon tissues were washed with phosphate-buffered saline for 6 times to remove feces and microbes, sliced into pieces, then cultured with serum-free RPMI 1640 medium with penicillin (1000 U/mL) and streptomycin (1000 U/mL) for 12 hours. The supernatant was collected by sequential centrifugation at 500 *g* for 10 minutes and 3000 *g* for 10 minutes. The levels of IL-1 $\beta$ , TNF- $\alpha$ , IL-6, IL-17A, GM-CSF, LIX, KC, MCP-1, MIP-2, IL-4, IFN- $\gamma$ , IL-4, IL-5, IL-10, IL-12, and IL-13 were measured by Multiplex Assays according to manufacturer's instructions (Merck, Darmstadt, Germany).

### TUNEL Staining

Sections of formalin-fixed, paraffin-embedded tissues were deparaffinized with xylene, rehydrated through graded ethanol. Cell death was detected by TUNEL Apoptosis Detection Kit (FITC) (40306E550; Yeasen, Shanghai, China) according to the manufacturer instructions. Five random fields (200×) were photographed and the average numbers of FITC-positive cells per field were presented.

### Measurement of Intestinal VP

Seven days after DSS treatment, mice were injected intravenously with 200- $\mu$ L Evans blue (0.5%, dissolved in phosphate-buffered saline). Thirty minutes later, mice were sacrificed and colons were photographed. Then, Evans blue in the colon was extracted by incubation at 65°C with formamide for 2 hours and determined spectrophotometrically at 630 nm against a standard curve.

### Miles Permeability Assay

Dulbecco's modified Eagle's medium or Fg supplemented with dimethyl sulfoxide or inhibitors (40  $\mu$ M or indicated concentrations) were injected intradermally into the abdomen. One hour later, mice were injected intravenously with 200- $\mu$ L Evans blue (0.5%, dissolved in phosphate-

buffered saline). Thirty minutes later, mice were sacrificed, and skins were dissected and photographed.

### G-Actin/F-Actin Assay

G-actin/F-actin fragmentation was performed by the G-actin/F-actin in vivo assay biochem kit (Cytoskeleton, Denver, CO) according to the manufacturer instructions.

### Statistical Analysis

Data from at least 3 independent experiments are shown as the mean  $\pm$  SEM. Mouse survival curves were constructed using the Kaplan-Meier product limit estimator and log rank (Mantel-Cox) test. Unless otherwise noted, the differences between 2 groups were analyzed by unpaired Student *t* test. Analyses were performed with Prism version 4.0 (GraphPad Software, San Diego, CA). All statistical tests were 2-sided and *P* < .05 was considered statistically significant.

All authors had access to the study data and had reviewed and approved the final article.

### References

1. Ungaro R, Mehandru S, Allen P, Peyrin-Biroulet L, Colombel J. Ulcerative colitis. *Lancet* 2017; 389:1756–1770.
2. Park-Windhol C, D'Amore PA. Disorders of vascular permeability. *Annu Rev Pathol* 2016;11:251–281.
3. Tolstanova G, Deng X, French S, Lungo W, Paunovic B, Khomenko T, Ahluwalia A, Kaplan T, Dacosta-Iyer M, Tarawski A, Szabo S, Sandor Z. Early endothelial damage and increased colonic vascular permeability in the development of experimental ulcerative colitis in rats and mice. *Lab Invest* 2012;92:9–21.
4. Sun BY, Yuan JY, Wang SY, Lin J, Zhang WJ, Shao JD, Wang RQ, Shi B, Hu HY. Qingchang suppository ameliorates colonic vascular permeability in dextran-sulfate-sodium-induced colitis. *Front Pharmacol* 2018;9:1235.
5. Taniguchi T, Inoue A, Okahisa T, Kimura T, Gohji T, Niki M, Kitamura S, Takeuchi H, Okamoto K, Kaji M, Okamura S, Takayama T, Nakasono M, Kudo E, Sano T. Increased angiogenesis and vascular permeability in patient with ulcerative colitis. *Gastrointest Endosc* 2009; 69:ab365.
6. Matsumoto K, Yamaba R, Inoue K, Utsumi D, Tsukahara T, Amagase K, Tominaga M, Kato S. Transient receptor potential vanilloid 4 channel regulates vascular endothelial permeability during colonic inflammation in dextran sulphate sodium-induced murine colitis. *Br J Pharmacol* 2018;175:84–99.
7. Kanazawa S, Tsunoda T, Onuma E, Majima T, Kagiya M, Kikuchi K. VEGF, basic-FGF, and TGF- $\beta$  in Crohn's disease and ulcerative colitis: a novel mechanism of chronic intestinal inflammation. *Am J Gastroenterol* 2001;96:822–8228.
8. Tolstanova G, Khomenko T, Deng X, Chen L, Tarawski A, Ahluwalia A, Szabo S, Sandor Z. Neutralizing anti-vascular endothelial growth factor (VEGF) antibody reduces severity of experimental ulcerative

- colitis in rats: direct evidence for the pathogenic role of VEGF. *J Pharmacol Exp Ther* 2009;328:749–757.
9. Cromer WE, Ganta CV, Patel M, Traylor J, Kevil CG, Alexander JS, Mathis JM. VEGF-A isoform modulation in an preclinical TNBS model of ulcerative colitis: protective effects of a VEGF164b therapy. *J Transl Med* 2013; 11:207.
  10. Davalos D, Akassoglou K. Fibrinogen as a key regulator of inflammation in disease. *Semin Immunopathol* 2012; 34:43–62.
  11. Millien VO, Lu W, Shaw J, Yuan XY, Mak G, Roberts L, Song LZ, Knight JM, Creighton CJ, Luong A, Kheradmand F, Corry DB. Cleavage of fibrinogen by proteinases elicits allergic responses through Toll-like receptor 4. *Science* 2013;341:792–796.
  12. Ryu J, Petersen M, Murray S, Baeten K, Meyer-Franke A, Chan J, Vagena E, Bedard C, Machado M, Rios Coronado P, Prod'homme T, Charo I, Lassmann H, Degen J, Zamvil S, Akassoglou K. Blood coagulation protein fibrinogen promotes autoimmunity and demyelination via chemokine release and antigen presentation. *Nat Commun* 2015;6:8164.
  13. Steinbrecher K, Horowitz N, Blevins E, Barney K, Shaw M, Harmel-Laws E, Finkelman F, Flick M, Pinkerton M, Talmage K, Kombrinck K, Witte D, Palumbo J. Colitis-associated cancer is dependent on the interplay between the hemostatic and inflammatory systems and supported by integrin alpha(M)beta(2) engagement of fibrinogen. *Cancer Res* 2010; 70:2634–2643.
  14. Zhang C, He A, Liu S, He Q, Luo Y, He Z, Chen Y, Tao A, Yan J. Inhibition of HtrA2 alleviated dextran sulfate sodium (DSS)-induced colitis by preventing necroptosis of intestinal epithelial cells. *Cell Death Dis* 2019;10:344.
  15. Plow E, Marguerie G, Ginsberg M. Fibrinogen, fibrinogen receptors, and the peptides that inhibit these interactions. *Biochem Pharmacol* 1987;36:4035–4040.
  16. Loike J, Sodeik B, Cao L, Leucona S, Weitz J, Detmers P, Wright S, Silverstein S. CD11c/CD18 on neutrophils recognizes a domain at the N terminus of the A alpha chain of fibrinogen. *Proc Natl Acad Sci U S A* 1991; 88:1044–1048.
  17. Redlich H, Vickers J, Lösche W, Heptinstall S, Kehrel B, Spangenberg P. Formation of platelet-leukocyte conjugates in whole blood. *Platelets* 1997;8:419–425.
  18. Pitkänen H, Jouppila A, Lemponen M, Ilmakunnas M, Ahonen J, Lassila R. Factor XIII deficiency enhances thrombin generation due to impaired fibrin polymerization - an effect corrected by factor XIII replacement. *Thromb Res* 2017;149:56–61.
  19. Neurath M. Cytokines in inflammatory bowel disease. *Nat Rev Immunol* 2014;14:329–342.
  20. Angelini DJ, Hyun SW, Grigoryev DN, Garg P, Gong P, Singh IS, Passaniti A, Hasday JD, Goldblum SE. TNF-alpha increases tyrosine phosphorylation of vascular endothelial cadherin and opens the paracellular pathway through fyn activation in human lung endothelia. *Am J Physiol Lung Cell Mol Physiol* 2006; 291:L1232–L1245.
  21. Dostert C, Grusdat M, Letellier E, Brenner D. The TNF family of ligands and receptors: communication modules in the immune system and beyond. *Physiol Rev* 2019; 99:115–160.
  22. Lominadze D, Dean W, Tyagi S, Roberts A. Mechanisms of fibrinogen-induced microvascular dysfunction during cardiovascular disease. *Acta Physiol (Oxf)* 2010; 198:1–13.
  23. Chen XL, Nam JO, Jean C, Lawson C, Walsh CT, Goka E, Lim ST, Tomar A, Tancioni I, Uryu S, Guan JL, Acevedo LM, Weis SM, Cheresh DA, Schlaepfer DD. VEGF-induced vascular permeability is mediated by FAK. *Dev Cell* 2012;22:146–157.
  24. Eliceiri BP, Paul R, Schwartzberg PL, Hood JD, Leng J, Cheresh DA. Selective requirement for Src kinases during VEGF-induced angiogenesis and vascular permeability. *Mol Cell* 1999;4:915–924.
  25. Weis SM, Cheresh DA. Pathophysiological consequences of VEGF-induced vascular permeability. *Nature* 2005;437:497–504.
  26. Fulton D, Gratton J, McCabe T, Fontana J, Fujio Y, Walsh K, Franke T, Papapetropoulos A, Sessa W. Regulation of endothelium-derived nitric oxide production by the protein kinase Akt. *Nature* 1999; 399:597–601.
  27. Chen J, Somanath PR, Razorenova O, Chen WS, Hay N, Bornstein P, Byzova TV. Akt1 regulates pathological angiogenesis, vascular maturation and permeability in vivo. *Nat Med* 2005;11:1188–1196.
  28. Thibeault S, Rautureau Y, Oubaha M, Faubert D, Wilkes BC, Delisle C, Gratton JP. S-Nitrosylation of beta-catenin by eNOS-derived NO promotes VEGF-induced endothelial cell permeability. *Mol Cell* 2010; 39:468–476.
  29. Di Lorenzo A, Lin M, Murata T, Landskroner-Eiger S, Schleicher M, Kothiya M, Iwakiri Y, Yu J, Huang P, Sessa W. eNOS-derived nitric oxide regulates endothelial barrier function through VE-cadherin and Rho GTPases. *J Cell Sci* 2013;126:5541–5552.
  30. Dudek S, Garcia J. Cytoskeletal regulation of pulmonary vascular permeability. *J Appl Physiol* 2001; 91:1487–1500.
  31. Lee TY, Gotlieb AI. Microfilaments and microtubules maintain endothelial integrity. *Microsc Res Tech* 2003; 60:115–127.
  32. Petrache I, Birukova A, Ramirez S, Garcia J, Verin A. The role of the microtubules in tumor necrosis factor-alpha-induced endothelial cell permeability. *Am J Respir Cell Mol Biol* 2003;28:574–581.
  33. Waschke J, Curry F, Adamson R, Drenckhahn D. Regulation of actin dynamics is critical for endothelial barrier functions. *American journal of physiology. Heart Circ Physiol* 2005;288:H1296–H1305.
  34. Morales-Ruiz M, Fulton D, Sowa G, Languino L, Fujio Y, Walsh K, Sessa W. Vascular endothelial growth factor-stimulated actin reorganization and migration of

endothelial cells is regulated via the serine/threonine kinase Akt. *Circ Res* 2000;86:892–896.

35. Enomoto A, Murakami H, Asai N, Morone N, Watanabe T, Kawai K, Murakumo Y, Usukura J, Kaibuchi K, Takahashi M. Akt/PKB regulates actin organization and cell motility via Girdin/APE. *Dev Cell* 2005;9:389–402.

---

Received July 23, 2020. Accepted October 14, 2020.

#### Correspondence

Address correspondence to: Jie Yan, PhD, The Second Affiliated Hospital, The State Key Laboratory of Respiratory Disease, Guangdong Provincial Key Laboratory of Allergy & Clinical Immunology, Guangzhou Medical University, 195 Dongfengxi Street, Yuexiu District, Guangzhou 510260, China. e-mail: [jieyan@gzhmu.edu.cn](mailto:jieyan@gzhmu.edu.cn); fax: 86-020-34153520. Ailin Tao, PhD, The Second Affiliated Hospital, The State Key Laboratory of Respiratory Disease, Guangdong Provincial Key Laboratory of Allergy & Clinical Immunology, Guangzhou Medical University, Guangzhou 510260, China. e-mail: [taoailin@gzhmu.edu.cn](mailto:taoailin@gzhmu.edu.cn); fax: 86-020-34153520.

#### CRediT Authorship Contributions

Jie Yan (Conceptualization: Equal; Data curation: Supporting; Formal analysis: Supporting; Funding acquisition: Lead; Investigation: Equal; Methodology: Supporting; Project administration: Supporting; Resources: Supporting; Software: Supporting; Supervision: Equal; Validation: Supporting; Visualization: Supporting; Writing – original draft: Supporting; Writing – review & editing: Equal)

Chong Zhang (Conceptualization: Lead; Data curation: Lead; Formal analysis: Lead; Funding acquisition: Supporting; Investigation: Lead; Methodology: Lead; Project administration: Lead; Resources: Equal; Software: Equal; Validation: Lead; Writing – original draft: Lead; Writing – review & editing: Lead)

Honglv Chen (Conceptualization: Supporting; Data curation: Equal; Formal analysis: Supporting; Project administration: Supporting; Resources: Supporting; Software: Equal; Supervision: Supporting; Validation: Supporting; Visualization: Equal; Writing – review & editing: Supporting)

Qiaoling He (Data curation: Supporting; Investigation: Supporting; Resources: Supporting; Software: Supporting; Supervision: Supporting; Validation: Supporting; Visualization: Supporting; Writing – review & editing: Supporting)

Yiqin Luo (Data curation: Supporting; Validation: Supporting; Writing – review & editing: Supporting)

Andong He (Data curation: Supporting; Validation: Supporting; Writing – review & editing: Supporting)

Ailin Tao (Conceptualization: Supporting; Funding acquisition: Equal; Supervision: Equal; Writing – review & editing: Supporting)

#### Conflicts of Interest

The authors disclose no conflicts.

#### Funding

This study was supported by grants from the Key Scientific Research Project of Colleges in Education Department of Guangdong Province (2018KZDXM057, J.Y.), the National Science and Technology Major Project of China (2016ZX08011-005, A.T.), Overseas Expertise Introduction Center for Discipline Innovation (111 center, D18010, J.Y.), Youth Program of Guangxi Natural Science Foundation of China (2019JJB140217, C.Z.), and Special Project Guangxi Science and Technology Base and Talent (2019AC20274, C.Z.).